Appendix DR1

1. Method of Statistical Analysis

One has to be careful and use only samples with complete Sm-Eu-Gd concentration data to study Eu/Eu* in the crust. This is because REEs are heterogeneous in the deep crust samples. Sm-Eu-Gd concentrations derived from different sets of crustal samples (e.g., Hacker et al., 2015) may not provide accurate Eu/Eu* estimates for the crust.

Concentrations of Sm, Eu and Gd in the UCC, MCC and LCC are significantly skewed by high concentration samples (Figure DR1). Logarithmic transformation fits these concentration data to Gaussian distribution (Figure DR2).

To calculate the mean concentrations of Sm, Eu and Gd and their associated uncertainties in the BCC, we used a bootstrapping resampling method. This technique allows estimation of the bulk composition and associated uncertainties with all samples taken into account. To do this, we first randomly resampled the UCC, MCC and LCC datasets. The size of each resample is equal to that of the original dataset. For example, our UCC dataset size is 328 (= 411*(1-20%)), and we resampled this dataset 328 times to make one UCC resample. For each resample, we calculated the mean Sm, Eu and Gd concentrations. Then we summed up the means of UCC, MCC and LCC resamples multiplied by their weighing factors (the mass proportions of the UCC, MCC and LCC). We repeated this step 100,000 times to get 100,000 resamples of mean BCC, with which we calculated the mean Sm, Eu, Gd concentrations and Eu/Eu* in the BCC (Figure DR3).

Table DR1. Lognormal means of Sm, Eu and Gd concentrations in the UCC, MCC and LCC. The asymmetrical uncertainties are two standard deviations of the populations.

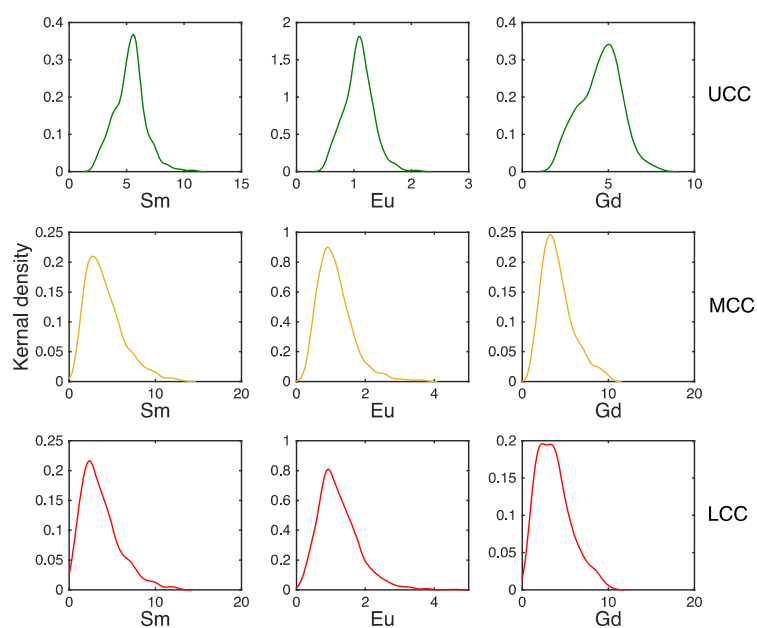|	UCC	MCC	LCC
Sm, ppm	$5.1^{+3.6}_{-2.1}$	$3.6^{+7.1}_{-2.4}$	$3.0^{+8.2}_{-2.2}$
Eu, ppm	$1.05^{+0.65}_{-0.40}$	$1.02^{+1.5}_{-0.6}$	$1.08^{+1.9}_{-0.7}$
Gd, ppm	$4.4^{+3.3}_{-1.9}$	$3.7^{+5.6}_{-2.2}$	$3.2^{+7.2}_{-2.2}$

Figure DR1. Distributions of Sm, Eu and Gd concentrations (ppm) in the UCC, MCC and LCC.
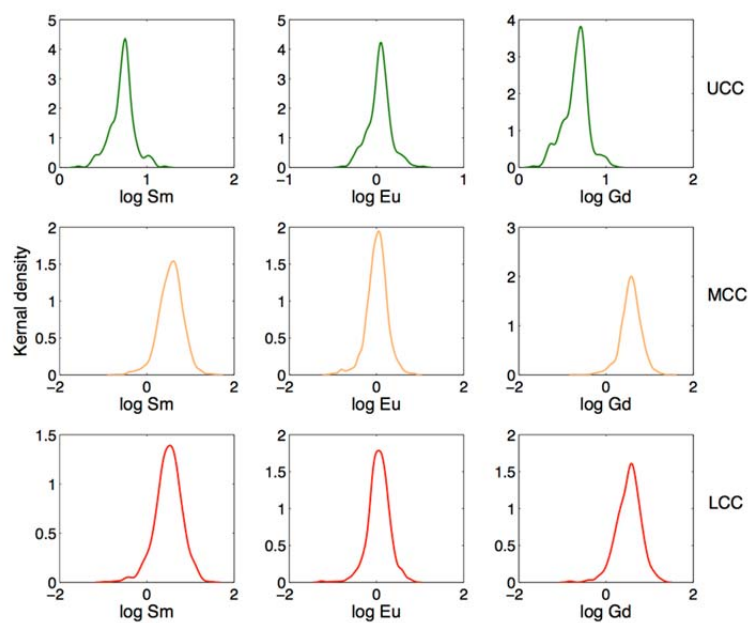

Figure DR2. Distributions of log-transformed Sm, Eu and Gd concentrations in the UCC, MCC and LCC.
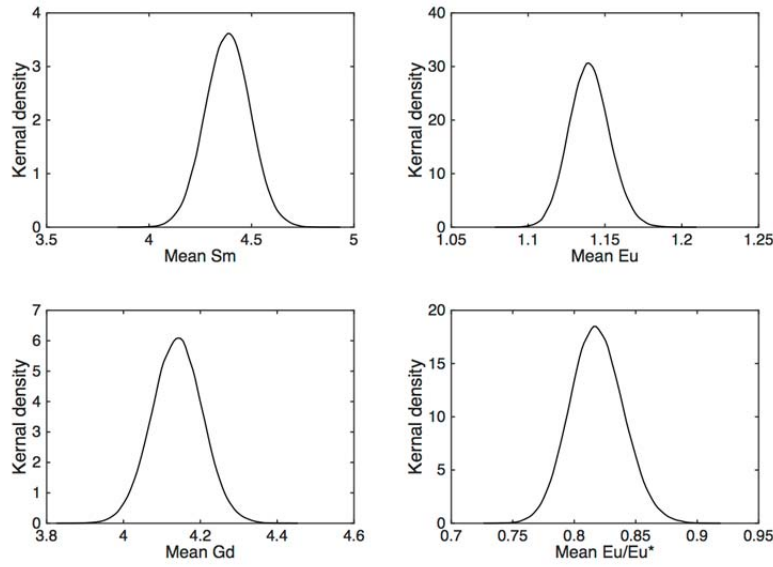
Figure DR3. Distributions of mean Sm, Eu and Gd concentrations (in ppm) and Eu/Eu* in the BCC.

We also simulated BCC samples and estimated the populations of Sm, Eu and Gd concentrations and Eu/Eu* in the simulated BCC samples. Each BCC sample is composed of one sample from the UCC, MCC and LCC, respectively, each of which was randomly selected from the UCC, MCC and LCC datasets and multiplied by the weighing factor. We obtained 100,000 simulated BCC samples by this scheme. The distributions of Sm, Eu, Gd concentrations and Eu/Eu* in the BCC samples are shown in Figure DR4.
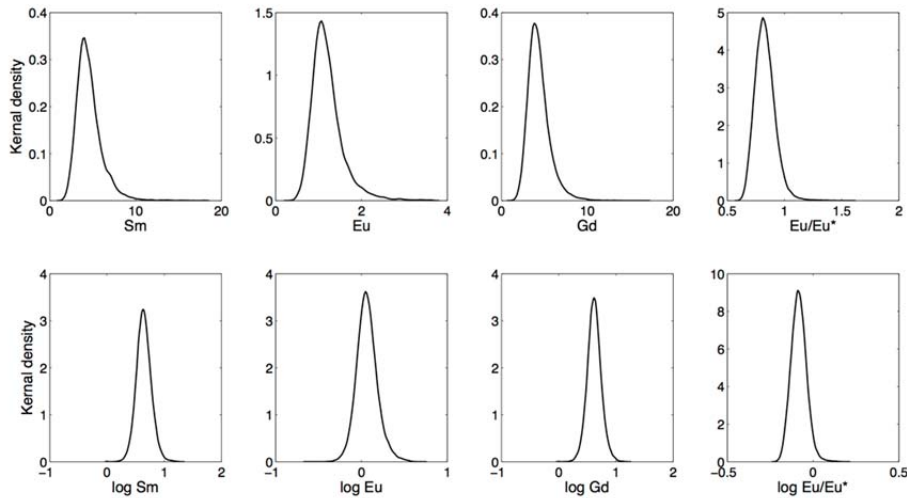

Figure DR4. Distributions of Sm, Eu, Gd concentrations (in ppm) and Eu/Eu* in the simulated BCC samples. Logarithmic transformation of the data resulted in Gaussian distributions.

2. Comparison of REE Patterns and Major Element Compositions of Various BCC Models
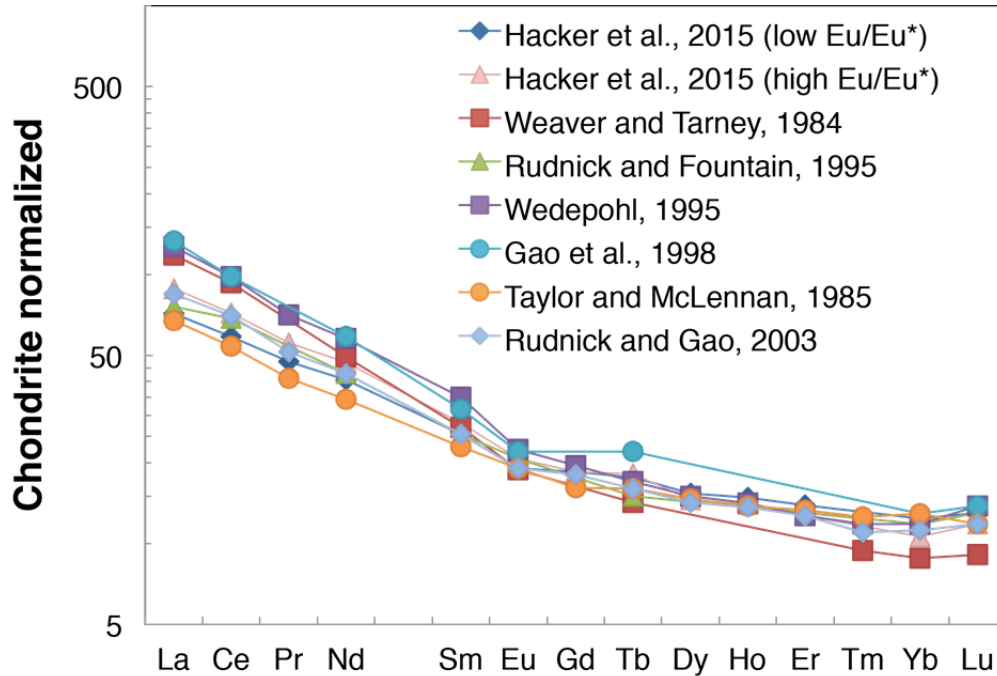

Figure DR5.

Published REE composition models for the BCC.

Table DR2. Bulk continental crust REE composition and Eu/Eu* of published models.

	Hacker et al., 2015 (low Eu/Eu*)	Hacker et al., 2015 (high Eu/Eu*)	Weaver and Tarney, 1984	Rudnick and Fountain, 1995	Wedepohl, 1995	Gao et al., 1998	Taylor and McLennan, 1985	Rudnick and Gao, 2003
La	17.0	21.0	28.0	18.0	30.1	31.5	16.0	20.0
Ce	36.0	44.0	57.0	42.0	60.0	60.0	33.0	43.0
Pr	4.5	5.3			6.7		3.9	4.9
Nd	19.0	22.0	23.0	20.0	27.0	27.4	16.0	20.0
Sm	3.9	4.3	4.1	3.9	5.4	4.8	3.5	3.9
Eu	1.1	1.2	1.1	1.2	1.3	1.3	1.1	1.1
Gd	3.8	3.8			4.0		3.3	3.7
Tb	0.66	0.68	0.5	0.6	0.6	0.8	0.6	0.6
Dy	3.9	3.7			3.8		3.7	3.6
Ho	0.84	0.79			0.80		0.78	0.77
Er	2.3	2.1			2.1		2.2	2.1
Tm			0.24		0.30		0.32	0.28
Yb	2.1	1.8	1.5	2.0	2.0	2.2	2.2	1.9
Lu	0.33	0.30	0.23	0.33	0.35	0.35	0.30	0.30
Eu/Eu*	0.87	0.91	0.86	0.97	0.86	0.78	0.99	0.89

Note: Eu/Eu* of BCC models that do not report Gd concentrations are calculated as Eu/Eu* = $Eu_N/(Sm_N^{2/3}*Tb_N^{1/3})$.

Table DR3. Lower crust major element compositions from this study (average of samples used to calculate Eu/Eu*) compared with previous studies. More studies of LCC major element compositions are available in Rudnick and Gao (2003). Errors are 2 σ_m.

	This study	Rudnick and Gao, 2003	Hacker et al., 2015 (mafic endmember)	Hacker et al., 2015 (felsic endmember)
SiO_2	53.3 ± 0.6	53.4	48.6	61.9
TiO_2	1.0 ± 0.1	0.82	1.40	0.78
Al_2O_3	16.3 ± 0.3	16.9	18.1	16.1
FeO_T	9.0 ± 0.3	8.57	10.44	6.52
MnO	0.18 ± 0.04	0.10	0.18	0.11
MgO	7.3 ± 0.4	7.24	6.87	3.14
CaO	8.9 ± 0.3	9.59	10.11	5.77
Na_2O	2.8 ± 0.1	2.65	2.85	3.92
K_2O	1.0 ± 0.1	0.61	1.22	1.54
P_2O_5	0.18 ± 0.01	0.10	0.23	0.21
Total	100	100	100	100

Table DR4. Middle crust major element compositions from this study (average of samples used to calculate Eu/Eu*) compared with previous studies. More studies of MCC major element compositions are available in Rudnick and Gao (2003). Errors are 2 σ_m.

	This study	Rudnick and Gao, 2003	Hacker et al., 2015 (mafic endmember)	Hacker et al., 2015 (felsic endmember)
SiO_2	60.1 ± 0.6	63.5	53.1	67.7
TiO_2	1.0 ± 0.1	0.69	1.26	0.55
Al_2O_3	15.2 ± 0.2	15.0	16.7	15.6
FeO_T	6.0 ± 0.3	6.02	10.32	4.46
MnO	0.16 ± 0.01	0.10	0.21	0.08
MgO	5.5 ± 0.2	3.59	5.98	1.72
CaO	7.5 ± 0.3	5.25	7.48	3.62
Na_2O	2.9 ± 0.1	3.39	3.38	3.88
K_2O	1.6 ± 0.1	2.30	1.29	2.26
P_2O_5	0.16 ± 0.01	0.15	0.24	0.18
Total	100	100	100	100

3. SensitivityTtests of How LCC Composition affects BCC Eu/Eu*

The amount of recycled lower continental crust is a function of the BCC Eu/Eu*, and our BCC has next to the lowest Eu/Eu* of existing compositional models (Table DR2, Fig. DR5). Because previous estimates of the BCC composition did not filter samples for reliability in calculations of Eu/Eu* (as described in section 1 of this appendix), and because most used log-normal means to calculate trace element abundances (e.g., Rudnick and Fountain, 1995; Rudnick and Gao, 2003, Hacker et al., 2015) these previous estimates cannot be used to determine how BCC composition affects the mass of recycled LCC. Instead, we have performed a series of sensitivity tests of our BCC composition, focusing on the LCC composition, which is the only portion of the crust to show a positive Eu anomaly. The LCC is highly heterogeneous, is also the least accessible, and arguably the poorest known in terms of bulk composition.

We investigate the variability of the LCC using the granulite database we have compiled for Eu/Eu*. We sorted these granulites by their Mg#, SiO_2 content, and mid-REE (Sm considered here) concentrations, and then calculated the running averages of

granulite composition (n = 100) as possible LCC compositions. Figure DR6 shows that the calculated BCC Eu/Eu* does not change beyond our uncertainty, no matter which flavor of granulite we adopt for the LCC. This demonstrates the robustness of BCC Eu/Eu* against the uncertainty in sampling of the LCC i.e., the proportion of mafic granulites to felsic granulites and high mid-REE granulites to low mid-REE granulites. This is due to the trade-off between Eu/Eu* and Eu concentration in granulites (Figure 2 in the paper). Generally, mafic granulites have higher Eu/Eu* but lower Eu concentrations than felsic granulites.
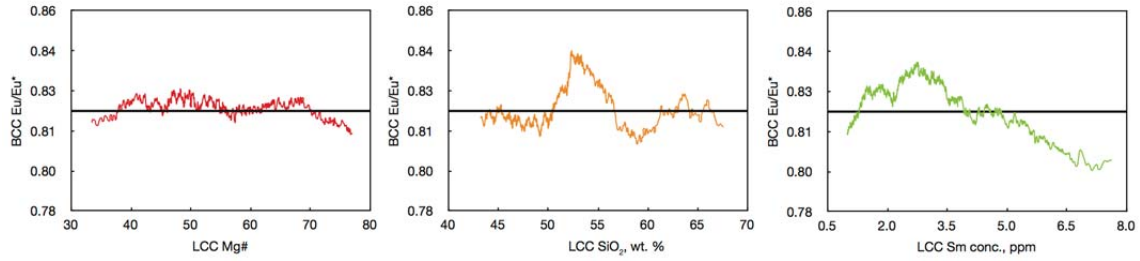

Figure DR6. BCC Eu/Eu* as functions of LCC Mg#, SiO_2 content and mid-REE (Sm considered here) concentration, respectively. The black lines (corresponding to Eu/Eu* = 0.82) indicate the BCC Eu/Eu* in Table 1 and the entire scale of the y-axis represents the adopted uncertainty of BCC Eu/Eu*.
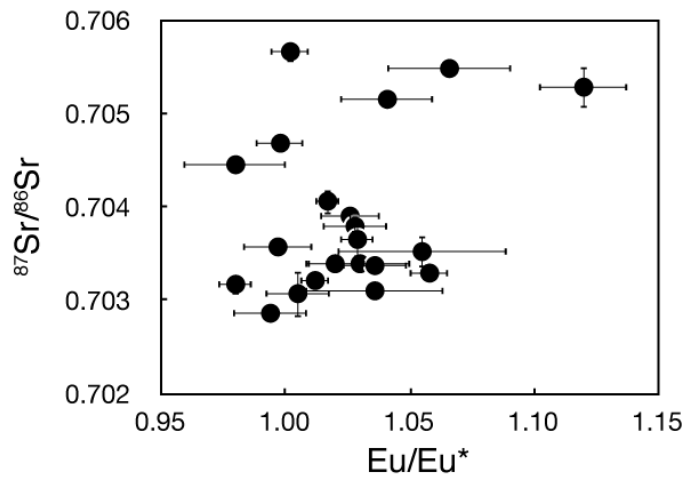
4. Eu/Eu* and Sr Isotopes in OIBs.

Figure DR7. $^{87}Sr/^{86}Sr$ vs. Eu/Eu* in OIB locality averages. Locality averages of Eu/Eu* are calculated using only OIBs with MgO > 10% to avoid any influence from shallow magma differentiation; locality averages of Sr isotopes are calculated using all samples from each ocean island system.

5. Mass Conservation Equations

$$Sm_{JCC} * m_{JCC} = Sm_{BCC} * m_{BCC} + Sm_{recycled\_LCC} * m_{recycled\_LCC} \qquad (A1)$$

$$Eu_{JCC} * m_{JCC} = Eu_{BCC} * m_{BCC} + Eu_{recycled\_LCC} * m_{recycled\_LCC} \qquad (A2)$$

$$Gd_{JCC} * m_{JCC} = Gd_{BCC} * m_{BCC} + Gd_{recycled\_LCC} * m_{recycled\_LCC} \qquad (A3)$$

$$m_{JCC} = m_{BCC} + m_{recycled\_LCC} \qquad (A4)$$

$$Eu/Eu*_{JCC} = \frac{(Eu_{JCC})_N}{\sqrt{(Sm_{JCC})_N * (Gd_{JCC})_N}} \geq 1 \qquad (A5)$$

The subscript N in equation A5 indicates chondrite value normalized.

References

Gao, S., Luo, T.-C., Zhang, B.-R., Zhang, H.-F., Han, Y.-w., Zhao, Z.-D., and Hu, Y.-K., 1998, Chemical composition of the continental crust as revealed by studies in East China: Geochimica et Cosmochimica Acta, v. 62, no. 11, p. 1959-1975.

Hacker, B. R., Kelemen, P. B., and Behn, M. D., 2015, Continental lower crust: Annual Reviews of Earth and Planetary Sciences, in press.

Hans Wedepohl, K., 1995, The composition of the continental crust: Geochimica et cosmochimica Acta, v. 59, no. 7, p. 1217-1232.

Rudnick, R., and Gao, S., 2003, Composition of the continental crust: Treatise on geochemistry, v. 3, p. 1-64.

Rudnick, R. L., and Fountain, D. M., 1995, Nature and composition of the continental crust: A lower crustal perspective: Reviews of Geophysics, v. 33, no. 3, p. 267-309.

Taylor, S. R., and McLennan, S. M., 1985, The Continental Crust, Wiley.

Weaver, B. L., and Tarney, J., 1984, Empirical approach to estimating the composition of the continental crust: Nature, v. 310, no. 5978, p. 575-577.

Appendix DR2 is available from the authors upon request.